



University of Southern Denmark

## Amorphous solid dispersion enhances permeation of poorly soluble ABT-102: True supersaturation vs. apparent solubility enhancement

Frank, Kerstin ; Brandl, Martin

*Published in:*  
International Journal of Pharmaceutics

*DOI:*  
10.1016/j.ijpharm.2012.08.014

*Publication date:*  
2012

*Document version:*  
Submitted manuscript

### *Citation for pulished version (APA):*

Frank, K., & Brandl, M. (2012). Amorphous solid dispersion enhances permeation of poorly soluble ABT-102: True supersaturation vs. apparent solubility enhancement. *International Journal of Pharmaceutics*, 437(1-2), 288-293. <https://doi.org/10.1016/j.ijpharm.2012.08.014>

Go to publication entry in University of Southern Denmark's Research Portal


### **Terms of use**

This work is brought to you by the University of Southern Denmark.  
Unless otherwise specified it has been shared according to the terms for self-archiving.  
If no other license is stated, these terms apply:

- You may download this work for personal use only.
- You may not further distribute the material or use it for any profit-making activity or commercial gain
- You may freely distribute the URL identifying this open access version

If you believe that this document breaches copyright please contact us providing details and we will investigate your claim.  
Please direct all enquiries to [puresupport@bib.sdu.dk](mailto:puresupport@bib.sdu.dk)

**AUTHOR QUERY FORM**

 <b>ELSEVIER</b>	<b>Journal:</b> IJP	<b>Please e-mail or fax your responses and any corrections to:</b>
	<b>Article Number:</b> 12805	<b>E-mail:</b> <a href="mailto:corrections.esch@elsevier.thomsondigital.com">corrections.esch@elsevier.thomsondigital.com</a>
	<b>Fax:</b> +353 6170 9272	

Dear Author,

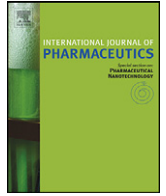
Please check your proof carefully and mark all corrections at the appropriate place in the proof (e.g., by using on-screen annotation in the PDF file) or compile them in a separate list. Note: if you opt to annotate the file with software other than Adobe Reader then please also highlight the appropriate place in the PDF file. To ensure fast publication of your paper please return your corrections within 48 hours.

For correction or revision of any artwork, please consult <http://www.elsevier.com/artworkinstructions>.

Any queries or remarks that have arisen during the processing of your manuscript are listed below and highlighted by flags in the proof. Click on the 'Q' link to go to the location in the proof.

<b>Location in article</b>	<b>Query / Remark: <a href="#">click on the Q link to go</a> Please insert your reply or correction at the corresponding line in the proof</b>
<a href="#">Q1</a> <a href="#">Q2</a>	<p>Please confirm that given names and surnames have been identified correctly. Please provide the volume number and page range for reference "Miller et al. (2012)".</p> <div style="border: 1px solid black; padding: 5px; margin-top: 20px;"> <p>Please check this box if you have no corrections to make to the PDF file <input type="checkbox"/></p> </div>

Thank you for your assistance.

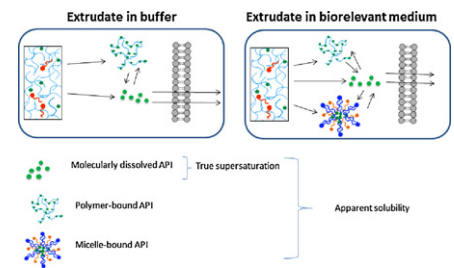


## Graphical Abstract

**Amorphous solid dispersion enhances permeation of poorly soluble ABT-102: True supersaturation vs. apparent solubility enhancement**

Kerstin J. Frank, Karin M. Rosenblatt, Ulrich Westedt, Peter Hölig, Jörg Rosenberg, Markus Mägerlein, Gert Fricker, Martin Brandl\*

International Journal of Pharmaceutics xx (2012) xxx–xxx



Contents lists available at [SciVerse ScienceDirect](http://www.elsevier.com/locate/ijpharm)

## International Journal of Pharmaceutics

journal homepage: [www.elsevier.com/locate/ijpharm](http://www.elsevier.com/locate/ijpharm)

# Amorphous solid dispersion enhances permeation of poorly soluble ABT-102: True supersaturation vs. apparent solubility enhancement

Kerstin J. Frank<sup>a,c</sup>, Karin M. Rosenblatt<sup>b</sup>, Ulrich Westedt<sup>b</sup>, Peter Hölig<sup>b</sup>, Jörg Rosenberg<sup>b</sup>, Markus Mägerlein<sup>b</sup>, Gert Fricker<sup>c</sup>, Martin Brandl<sup>a,\*</sup>

<sup>a</sup> Institute of Physics, Chemistry and Pharmacy, University of Southern Denmark, Campusvej 55, DK-5230 Odense M, Denmark

<sup>b</sup> Abbott GmbH & Co. KG, Knollstrasse 50, D-67061 Ludwigshafen, Germany

<sup>c</sup> Dept. of Pharmaceutical Technology, Institute of Pharmacy and Molecular Biotechnology, University of Heidelberg, Im Neuenheimer Feld 366, D-69120 Heidelberg, Germany

## ARTICLE INFO

## Article history:

Received 10 June 2012

Received in revised form 5 August 2012

Accepted 9 August 2012

Available online xxx

## Keywords:

Permeability  
Solid dispersion  
Solubility  
Supersaturation  
FaSSiF

## ABSTRACT

Amorphous solid dispersions (ASDs) represent a promising formulation approach for poorly soluble drugs. We explored the formulation-related impact of ASDs on permeation rate, apparent solubility and molecular solubility of the poorly soluble drug ABT-102. The influence of fasted state simulated intestinal fluid (FaSSiF) as dispersion medium was also studied.

ASDs were prepared by hot-melt extrusion. Permeation rate was assessed by the Caco-2 transwell assay. Cell viability and barrier integrity were assured by AlamarBlue®, TEER and permeability of the hydrophilic marker carboxyfluorescein. Apparent solubility and molecular solubility were evaluated by using centrifugation and inverse dialysis, respectively.

The in vitro permeation rate of ABT-102 from aqueous dispersions of the ASD was found 4 times faster than that from the dispersions of the crystals, while apparent solubility and molecular solubility of ABT-102 were increased. Yet, a further increase in apparent solubility due to micellar solubilization as observed when dispersing the ASD in FaSSiF, did not affect molecular solubility or permeation rate.

Overall, a good correlation between permeation rate and molecular solubility but not apparent solubility was seen.

© 2012 Published by Elsevier B.V.

## 1. Introduction

Increasingly, modern drug candidates tend to be poorly soluble. Many of them belong to class II of the Biopharmaceutical Classification System (BCS), which predicts the intestinal absorption of a given drug, based on its solubility and permeation across Caco-2 (Amidon et al., 1995). Class II comprises compounds of poor solubility but high permeability. Bioavailability of such BCS II compounds is restricted by their solubility. During the last years, various advanced oral formulation strategies have been used to enhance solubility and/or dissolution rate of poorly soluble active pharmaceutical ingredients (APIs), such as self (micro)emulsifying drug delivery systems (S(M)EDDS), microemulsions, nanocrystals, mesoporous silica and solid dispersions. It is controversially discussed, however, if and how these strategies enhance bioavailability (Singh et al., 2011).

In a previous study, we investigated how the inclusion of the poorly soluble ABT-102 (TRPV1 antagonist (Kym et al., 2009))

(chemical structure and characteristics (Frank et al., 2012)) into taurocholate/phosphatidylcholine micelles, contained in simulated intestinal fluid, affects apparent solubility and permeation rate across Caco-2 in the case of dispersions of the API. Furthermore, a method was developed to determine the molecular solubility in the presence of micelles. It was seen that neither the permeation rate nor the concentration of molecularly dissolved drug were increased in the presence of the micelles, even though the micelles induced a remarkable increase in apparent solubility.

In the present study we focused on ASDs generated by hot melt extrusion, which have been described to have a positive effect on bioavailability of poorly soluble drugs (Breitenbach, 2002; Leuner and Dressman, 2000; Vasconcelos et al., 2007). Typically, the amorphous drug is imbedded in a polymer matrix (solid dispersion) or the drug is molecularly dispersed in the polymer matrix (solid solution). Both systems contain the drug in its high energy state (Brouwers et al., 2009; Janssens and Van den Mooter, 2009). Typically, ASDs contain surfactants, which act as plasticizers and crystallization inhibitors during production and in the solid state of the ASDs. Furthermore, they serve as wetting agents, precipitation inhibitors or solubilizing agents in the aqueous dispersions of ASDs (Brouwers et al., 2009; Overhoff et al., 2008).

\* Corresponding author at: FKF, SDU, Campusvej 55, 5230 Odense C, Denmark.  
Tel.: +45 6550 2525; fax: +45 6615 8780.

E-mail address: [mmb@ifk.sdu.dk](mailto:mmb@ifk.sdu.dk) (M. Brandl).

**Table 1**  
Composition of the extrudate formulation F1 and the corresponding placebo extrudate (API-free formulation F1).

Ingredients	F1 percentage [%]	Placebo percentage [%]
ABT-102	5	—
Copovidon Typ K28 (Kollidon <sup>®</sup> VA 64)	81.5	85.7
Sucrose palmitate (Surfhope <sup>®</sup> D-1615)	1.5	1.6
Poloxamer 188 (Pluronic <sup>®</sup> F68)	6.0	6.3
Polysorbate 80 (Tween 80 <sup>®</sup> )	5.0	5.3
Fumed silica (Aerosil 200 <sup>®</sup> )	1.0	1.1

The aim of the current study was to investigate an aqueous dispersion of an ASD of the poorly soluble compound ABT-102 in terms of apparent and molecular solubility, as well as permeation rate. The ASD examined here consisted of the poorly soluble ABT-102, a hydrophilic polymer, and three surfactants.

## 2. Materials and methods

### 2.1. Materials

ABT-102 (chemical structure and physicochemical properties published by Frank et al., 2012) as well as the ASDs (F1 and placebo extrudate; compositions: Table 1) were provided by Abbott GmbH & Co. KG (Ludwigshafen, Germany). A general description of the preparation method is given by Breitenbach (2002). Hanks balanced buffered salt solution (washing and dispersion medium) and supplementary salts MgSO<sub>4</sub>·7H<sub>2</sub>O, NaHCO<sub>3</sub> and CaCl<sub>2</sub>·2H<sub>2</sub>O (HBSS++) were obtained from Sigma-Aldrich Chemie GmbH (Munich, Germany). FaSSiF was prepared by dispersing SIF instant powder (Phares Drug Delivery AG, Muttenz, Switzerland) containing taurocholate and lecithin (ratio 4:1) in the FaSSiF blank buffer.

For cell culturing, Dulbecco's modified Eagle's medium (DMEM), supplemented with fetal bovine serum (FBS) and other additional ingredients (see Section 2.2.3) were utilized (all Biochrom AG, Berlin, Germany). Rat tail collagen was purchased from Roche Pharma AG (Mannheim, Germany). Bovine serum albumin (BSA), acetonitrile (ACN), Triton X-100, trifluoroacetic acid (TFA), NaOH, NaCl and NaH<sub>2</sub>PO<sub>4</sub>·H<sub>2</sub>O were obtained from Sigma-Aldrich Chemie GmbH.

### 2.2. Methods

#### 2.2.1. Powder X-ray diffraction

The ASD was investigated for crystalline parts of ABT-102 using powder X-ray diffraction. Diffraction patterns were recorded using a Panalytical X'Pert Pro MPD diffractometer (Panalytical, Eindhoven, Netherlands) with a Pixel detector, Data Collector and High Score software. Measurements were performed with a Cu K $\alpha$  radiation source at 40 kV voltage and 40 mA current from 2.5 $\lambda$  to 3.2 $\lambda$  2-theta in a continuous scanning mode. This range was chosen as the biggest reflex was seen to be at 2.9 $\lambda$  2-theta (supplementary data). The instrument was set to a step width of 0.006 $\lambda$  2-theta and a measurement time per step of 3000 s. The irradiated sample length was 20 mm.

Sample preparation was done by milling approximately 1.5 g of ASD with a ball mill (Pulverisette 23, Fritsch, Idar-Oberstein, Germany) at 30 Hz for 30 s. A frontloading 35 mm diameter powder diffraction sample holder (Panalytical) was used for the

measurements and the sample was covered with a Polyimide (Kapton) film (Chemplex, Palm City, FL, USA).

#### 2.2.2. Preparation of dispersions

Sample dispersions were prepared by dispersing the ASDs (beads) or crystalline ABT-102 in HBSS++ or FaSSiF in a volumetric flask (magnetic stirring at 400 rpm for 1 h at 37 $\lambda$  C).

#### 2.2.3. Apparent solubility

Sample dispersions were prepared as described in Section 2.2.2. Afterwards a defined volume of the aqueous dispersions was transferred into centrifugation tubes, which were centrifuged for 60 min at 18,500  $\times$  g at 37 $\lambda$  C (J2-MC, Beckman). These settings were chosen, because the turbidity reached a plateau after 55 min of centrifugation at 18,500  $\times$  g i.e., all big particles are expected to be spun down at that time point. After centrifugation, aliquots of the supernatant were withdrawn, immediately diluted with acetonitrile and analyzed via HPLC-UV/Vis, as described in Section 2.2.9.

The centrifugation approach was found inappropriate for determination of the apparent solubility of the placebo extrudate plus crystalline ABT-102 due to floating particles. Thus, for this sample, separation of particles was performed by membrane filtration (pore size 0.2  $\mu$ m, CA-membrane filter, Buch&Holm, Herlev, Denmark).

#### 2.2.4. Quantification of molecularly dissolved ABT-102

The method has been described by Frank et al. (2012). In brief, the sample dispersion (prepared as described in Section 2.2.2) was transferred into a beaker (donor; V = 200 ml). Then, Midi GeBAflex dialysis tubes (3.5 kDa cut-off, Gene Bioapplication L.T.D., Yavne, Israel) filled with 800  $\mu$ l of HBSS++ or FaSSiF blank buffer (both at 37 $\lambda$  C) (acceptor) were put into the sponge-like floating device and set into the beaker. The beaker was incubated in a shaking water bath (Julabo SW23, Buch & Holm, Herlev, Denmark) at 37 $\lambda$  C and 50 rpm. Samples were drawn from inside the dialysis vials (acceptor) under equilibrium conditions, diluted with ACN and analyzed as described in Section 2.2.9. Preliminary experiments indicated that equilibrium was achieved after 20 h, and adsorptive drug-loss was marginal (data not shown).

#### 2.2.5. Caco-2 cell culture

DMEM, supplemented with 10% FBS, 1% non-essential amino acid, 1% penicillin-G, 1% streptomycin and 0.5% ciprofloxacin was used as cell culture medium. Caco-2 cells (Rockville type) were supplied with fresh medium every other day and passaged weekly. For experiments, cells between passage numbers 46 and 75 were utilized. Cells were seeded on pre-coated (rat tail collagen) 12-well transwell or 96-well plates (Corning GmbH, Life Sciences, Wiesbaden, Germany) with a density of approximately 75 000/cm<sup>2</sup> and cultivated for 14–16 days at 37 $\lambda$  C in 5% CO<sub>2</sub>, until a confluent monolayer was achieved.

#### 2.2.6. Cytotoxicity

For evaluation of cytotoxicity, AlamarBlue<sup>®</sup> (Invitrogen, Carlsbad, CA, USA), assay was applied. Culture medium was removed, cells were washed twice with HBSS++ and then sample dispersions were added. After incubating for 3.5 h at 37 $\lambda$  C, the sample dispersions were discarded, cells were washed again with pre-warmed HBSS++ and the testing reagent AlamarBlue<sup>®</sup> was added. Cells were incubated for another 2 h and then fluorescence was measured using a fluorescence plate reader (Fluoroscan Ascent, LabSystems GmbH, Frankfurt, Germany). Fluorescence of sample treated cells was expressed as a ratio relative to the negative control (HBSS++).

#### 2.2.7. Barrier integrity

Culture medium was first removed and then cells were washed twice with HBSS++. Thereafter, inserts were set in the cellZscope<sup>®</sup>

device (nanoAnalytics GmbH, Münster, Germany), HBSS++ was added apically and basolaterally. Next, transepithelial electrical resistance (TEER) was measured. After equilibration (approx. 60 min), apical HBSS++ was replaced with sample dispersions and incubated for up to 3.5 h. Throughout the course of the incubation, TEER of all 12 inserts was measured. In addition to the TEER measurements, carboxyfluorescein (CF) was added to the sample dispersions as hydrophilic marker (20  $\mu\text{M}$ ) and its permeability was evaluated. Samples were withdrawn at five time points from the basolateral side and the concentration of carboxyfluorescein (CF) in the acceptor was measured using a fluorescence plate reader (Fluoroscan Ascent, Labsystems GmbH, Frankfurt, Germany).

### 2.2.8. Permeation rate

For evaluation of the permeation rate of ABT-102 across the cell monolayer, cells were treated as described in Section 2.2.5. BSA ( $c=4\%$ , w/w) was added to HBSS++ on the basolateral side to maintain sink conditions and to saturate unspecific binding sites. This procedure has been described in the literature for performing permeation rate studies with poorly soluble APIs (Buckley et al., 2012; Hubatsch et al., 2007).

A three-fold volume of acetonitrile was added to the samples from the acceptor side to precipitate the protein. Next, samples were vortexed, followed by centrifugation for 10 min at 10 000 rpm (CF 5415D, Eppendorf AG, Hamburg, Germany). Upon precipitation of BSA, the supernatant was immediately analyzed by HPLC-UV-vis (see Section 2.2.9).

The normalized permeation rate ( $J$ ) was calculated with the formula  $J = (1/A) \times (dc/dt)$ , where  $A$  represents the surface area of the filter and  $dc/dt$  the permeation rate.

### 2.2.9. Quantification of ABT-102 by HPLC-UV-vis

The instrument consisted of a separation unit (Ultimate 3000, Dionex Co., Sunnyvale, USA) with a Dionex C18 column (4.6 mm  $\times$  300 mm) coupled to a UV/Vis detector (Ultimate 3000, Dionex Co., Sunnyvale, USA). Measurements were performed at a flow rate of 1.5 ml/min with a gradient, starting with 45% of eluent A (0.1% TFA in water) and 55% of eluent B (0.1% TFA in ACN), shifting to 20% of eluent A and 80% of eluent B over 10 min, followed by 3 min of isocratic flow profile. The injection volume was 100  $\mu\text{l}$ . For the analysis of the samples, freshly prepared calibration curves were used ( $R^2 \geq 0.998$ ) and quality controls were run after every 10–20 samples to ensure accuracy of the method throughout the whole sequence.

### 2.2.10. Data analysis

Comparison of two data sets was performed by using unpaired Student's  $t$ -test (two tailed).  $p \leq 0.05$  was considered as significantly different.

## 3. Results

### 3.1. Permeation rate

Aqueous dispersions (in HBSS++) of the ASD F1 (composition Table 1) were investigated in terms of the permeation rate of ABT-102 across the cell monolayer (Fig. 1). The obtained permeation rate values were compared to these of dispersions of crystalline ABT-102 in HBSS++, published recently by Frank et al. (2012).

The dispersion of F1 in HBSS++ yielded significantly higher ABT-102 permeation rates than crystalline ABT-102. Furthermore, there was no significant difference observed when FaSSIF was used as dispersion medium of F1 instead of HBSS++ (Fig. 1). The flux of crystalline ABT-102, dispersed in FaSSIF, was investigated in a previous study and found to be not significantly different from the flux

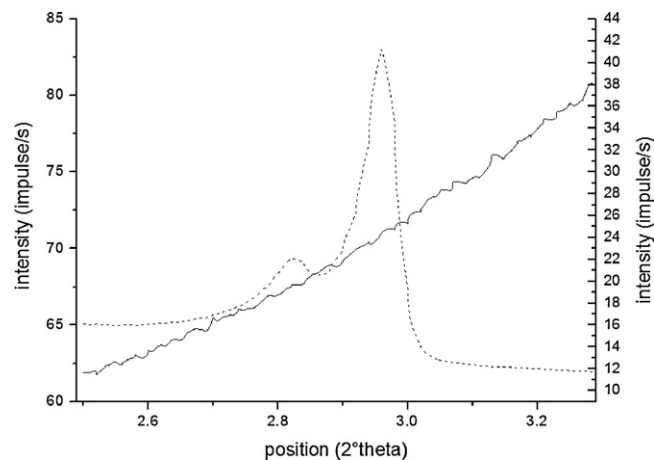


Fig. 1. Caco-2 permeation rates: Normalized flux (divided by area of filter surface) of dispersions of ABT-102 crystals in HBSS++ ( $n=5$ ; mean  $\pm$  SD) and of dispersions of the ASD F1 ( $n=8$ ; mean  $\pm$  SD) in HBSS++ and FaSSIF. \* Significance calculated by unpaired Student's  $t$ -test ( $p \leq 0.05$ ).

of the ABT-102 crystals dispersed in HBSS++, despite the up to 40 times increased apparent solubility (Frank et al., 2012).

In order to investigate if the observed enhanced permeation rate in the case of the ASD was due to the interaction(s) of excipient(s) with the Caco-2-barrier, various control-experiments were performed:

The AlamarBlue<sup>®</sup> assay was used to assess cytotoxicity of F1 as well as the permeability of carboxyfluorescein (CF) to determine if F1 had a deleterious effect on the membrane's barrier function (Table 2). In both experiments, HBSS++ was used as negative control and Triton X-100 (1% solution), well known for its cell damaging effect, as positive control. None of the samples showed a cytotoxic effect. The  $P_{app}$  values of the hydrophilic CF in the presence of the sample dispersions were not significantly different in comparison to the negative control.

Furthermore, using cellZscope<sup>®</sup>, it was possible to monitor the TEER throughout the entire course of incubation. There was an initial drop of the TEER values observed for all sample dispersions (and the negative control), but the TEER increased again to the initial starting value. This drop was probably due to the stress, which the cells experienced because of the aspiration of buffer and addition of the samples. Only in case of the positive control Triton X-100, was the resistance close to zero (Fig. 2).

In conclusion, a toxic or damaging effect of the sample dispersions on the cell monolayer could be ruled out.

Tween 80 is known to have a P-gp inhibiting effect and therefore might alter the permeation rate of a P-gp substrate. However, ABT-102 has recently been found to be no substrate of the efflux pump P-gp (Frank et al., 2012). P-gp inhibition thus is not likely to be the reason for increased ABT-102 permeation rate from the ASD F1.

### 3.2. Characterization of the solid state

ASDs are regarded as promising in terms of enhancing bioavailability of poorly soluble drugs under the prerequisite that either a dispersion of the amorphous ABT-102 in the polymer matrix (amorphous solid dispersion) or a solid solution (molecular dispersion) is generated (Brouwers et al., 2009). Powder X-ray scattering was performed in order to check the presence of drug crystallites in the ASD. The diffractogram in Fig. 3 indicates the absence of crystalline ABT-102 in F1.

**Table 2**  
Influence of the ASD formulation F1, dispersed in HBSS++ and in FaSSIF, on cell viability and on the integrity of the cell monolayer. (a) Cell viability: AlamarBlue® test; mean ± SD ( $n \geq 16$ ). (b) Integrity of the cell monolayer: Carboxyfluorescein permeability; mean ± SD ( $n \geq 4$ ).

	(a) AlamarBlue® test		(b) Carboxyfluorescein permeability	
	Viability [%]	Significance <sup>a</sup>	$P_{app}$ [ $\times 10^{-6}$ cm/s]	Significance <sup>a</sup>
HBSS++	100.0 ± 3.3	Reference	0.17 ± 0.08	Reference
Formulation F 1 in HBSS++	101.7 ± 5.9	No	0.15 ± 0.09	No
Formulation F1 in FaSSIF	97.0 ± 5.1	No	0.27 ± 0.07	No
Triton X-100 1%	2.7 ± 0.1	Yes	11.40 ± 1.80	Yes

<sup>a</sup> Significance calculated by unpaired Student's *t*-test ( $p \leq 0.05$ ).

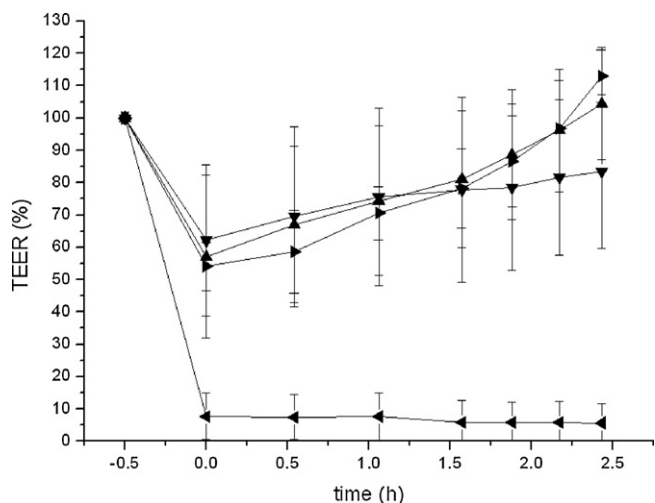


**Fig. 2.** Transepithelial electrical resistance measurement: TEER (%) related to measured TEER before incubation with sample dispersions on the apical sides ( $n = 3-5$ , mean ± SD). All starting values were  $>250 \Omega \text{ cm}^2$ . —●— F1 in FaSSIF; —▲— F1 in HBSS++; —○— Triton-X (positive control); —▶— HBSS++ (negative control).

### 3.3. Apparent and molecular solubility

We determined apparent and molecular solubility of ABT-102 in dispersions of F1 in HBSS++ as well as of F1 in FaSSIF.

First, apparent solubility was investigated. Non-dissolved material (particles) in the dispersions of the ASD was separated by centrifugation. The concentration of ABT-102 in the clear to opalescent supernatant was quantified. Apparent solubility was found to be enhanced up to 10 times in case of the dispersion of F1 in HBSS++, in comparison to the crystalline form of ABT-102. Furthermore,

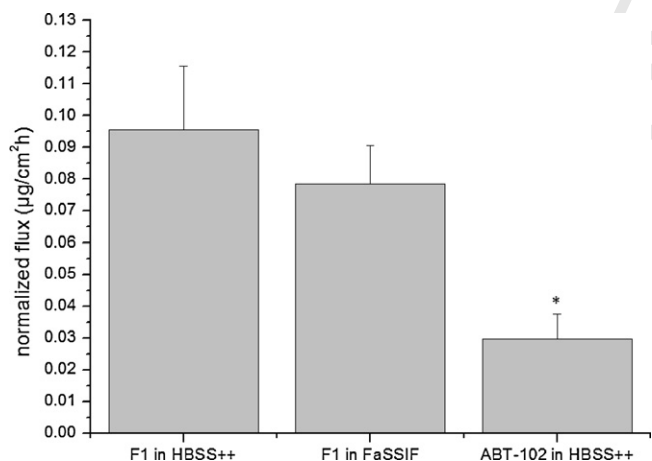


**Fig. 3.** Powder X-ray diffractogram: small angle X-ray scattering of the extrudate formulation F1 (solid; right y-axis) and of the placebo extrudate (F1 without ABT-102), spiked with crystalline ABT-102 (dotted; left y-axis).

the apparent solubility of the crystalline ABT-102 alone was in the same magnitude as a mixture containing crystalline ABT-102 plus placebo extrudate. FaSSIF as dispersion medium further increased the apparent solubility of ABT-102 in dispersions of F1 (100-fold) in comparison to the crystalline ABT-102 in HBSS++. It has been reported in the literature, that the taurocholate and the lecithin, which are present in FaSSIF, generate micelles that may enhance the solubility of poorly soluble APIs (Schwebel et al., 2011).

Inverse dialysis was performed to determine the concentration of molecularly dissolved ABT-102. The cut-off (3500 Da) was chosen such that only molecularly dissolved ABT-102 could pass, not micellar-bound or nanoparticulate one. Table 3 shows the molecular solubility of ABT-102 in dispersions of the ASD F1 and of crystalline ABT-102 in HBSS++ and in FaSSIF.

In the case of F1 dispersed in HBSS++, the molecular solubility of ABT-102 was found to be doubled in comparison to the one of crystalline ABT-102 (solubility limit). This indicates that dispersing F1 resulted in “true” supersaturation of the ABT-102. Inverse dialysis of a physical mixture, containing placebo extrudate plus crystalline ABT-102, dispersed in HBSS++ did not reveal an increase in the concentrations of molecularly dissolved ABT-102. Obviously, supersaturation is not related to the mere presence of the excipients. Interestingly, the same extent of “true” supersaturation (i.e. enhanced molecular solubility of ABT-102) is observed in FaSSIF as compared to HBSS++.

## 4. Discussion

The apparent solubility of the ABT-102 containing ASD (F1) in HBSS++ was ten times higher than that of crystalline ABT-102. In addition, the apparent solubility was higher in FaSSIF as compared to buffer, most likely due to micellar solubilization (Schwebel et al., 2011). This indicates two different solubility enhancement mechanisms, one related to the amorphous solid dispersion and one related to FaSSIF. The two effects appear to coexist. The apparent solubility of the physical mixture of the placebo extrudate and ABT-102 crystals was in the same range as the apparent solubility of ABT-102 crystals in HBSS++ alone. Micellar drug solubilization by the three surfactants present in the ASD was thus ruled out. Furthermore, the concentrations of the surfactants in the dispersion of the ASD (at the given concentration) are close to, or well below, the

**Table 3**

Solubility of ABT-102. Apparent solubility: Concentrations of ABT-102 in the supernatant after centrifugation of the sample dispersions ( $n = 6-7$ , mean ± SD). Molecular solubility: Concentrations of molecularly dissolved ABT-102 in the sample dispersions, assessed by inverse dialysis ( $n = 4-6$ , mean ± SD).

	Apparent solubility [ $\mu\text{g/ml}$ ]	Molecular solubility [ $\mu\text{g/ml}$ ]
F1 in HBSS++	0.58 ± 0.08	0.15 ± 0.01
F1 in FaSSIF	5.43 ± 0.41	0.16 ± 0.01
ABT-102 in HBSS++	0.05 ± 0.01	0.09 ± 0.01
ABT-102 in FaSSIF++	2.11 ± 0.28	0.08 ± 0.01
ABT-102 + placebo extrudate in HBSS++	0.06 ± 0.01	0.08 ± 0.01

critical micellar concentrations of these surfactants that are given in literature (polysorbate 80: Dawson et al., 1989; sucrose palmitate: Becerra et al., 2006; poloxamer 188: Cheng et al., 2012). Hence, it is assumed that there are no micelles generated.

Interestingly, molecular solubility was only found increased by a factor of two in the dispersions of the ASD, irrespective of the dispersion medium (FaSSiF or HBSS++), indicating “true” supersaturation. In contrast, a physical mixture of the placebo extrudate with the crystalline ABT-102 did not influence molecular solubility. This led us to the conclusion that the increase in molecular solubility is a consequence of the amorphous state of the ABT-102 in the hot melt extrudate. At the same time this rules out potential artifacts caused by surfactants, passing the dialysis membrane and generating solubilizing micelles inside the dialysis vials.

Although it has been repeatedly hypothesized in literature that ASDs may generate supersaturation (Brouwers et al., 2009; Linn et al., 2012; Miller et al., 2012), the results presented here are to our knowledge the first experimental proof that molecular solubility is enhanced (“true” supersaturation) in aqueous dispersions of ASDs, even in the presence of FaSSiF micelles.

Previous literature reported apparent solubility data, which does not distinguish between molecular solubility and colloidal solubilization through micelle- or polymer-association. Nevertheless a reasonable correlation between supersaturation data gained this way, and bioavailability enhancement has been found in cases where supersaturation is induced/stabilized by mesoporous silica and/or polymers: Van Speybroeck et al. (2010b) quantified supersaturation of mesoporous silica formulations combined with polymers using 0.45  $\mu\text{m}$  pore size membrane filtration, and found reasonable correlation with rat bioavailability data. In another study, Van Speybroeck et al. (2010a) correlated in vitro release of various mesoporous silica formulations (filter pore size 0.1  $\mu\text{m}$ ) with rat bioavailability data, which showed a good correlation between AUCs of the dissolution profiles and the plasma curves.

For surfactant-containing formulations, however, there appear to be discrepancies between supersaturation/apparent solubility and bioavailability: Do et al. (2011) compared apparent solubility (using filtration, pore size 0.45  $\mu\text{m}$ ) of various “supersaturating” fenofibrate formulations (micellar solubilization), with rat AUC and  $C_{\text{max}}$  and concluded that they were in disagreement. A dissolution/permeation system was used by Buch et al. (2010b) to evaluate both dissolution and permeation across a Caco-2 cell monolayer of 5 “supersaturating formulations”. In their data set, fraction dissolved (filtrated 0.2  $\mu\text{m}$ ) showed only moderate correlation with in vitro permeability as well as rat bioavailability. Interestingly, Buch et al. (2010a) corrected apparent solubility values generated by centrifugation, with fraction permeated through 10 kDa membranes and found surfactant-dependent correlation with human bioavailability. They explained their observation by a surfactant-specific interaction with FaSSiF micelles. Permeation from dispersions of ASDs containing surfactants has recently been shown to be enhanced as compared to the crystalline API (Kanzler et al., 2010). However, apparent solubility or molecular solubility was not evaluated at the same time.

In general, passive permeation of poorly soluble and well permeable drugs should increase with increasing concentrations of dissolved drug. More recently, several reports indicated that colloidal solubilized drug may not be available for permeation (Fischer et al., 2011; Frank et al., 2012; Ingels et al., 2004). Therefore, we correlated permeation rates with apparent solubilities and molecular solubilities (Fig. 4). Our data indicate that in this case “true” supersaturation appears to correlate with enhanced permeation rate, while increase in apparent solubility due to micellar solubilization appears to have little or no impact on permeation rate. One should bear in mind, that due to experimental constraints (long equilibration times needed for inverse dialysis), the molecularly

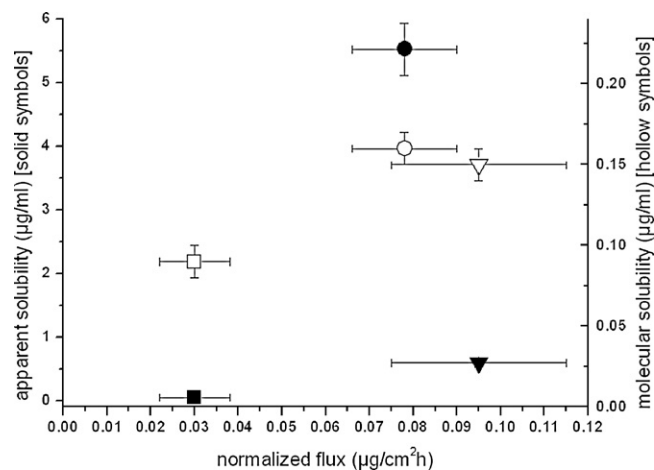


Fig. 4. Correlation plot: Normalized flux (x-axis) plotted against apparent solubility (left y-axis; solid symbols) and molecular solubility (right y-axis; hollow symbols). Quadrangle: crystals in HBSS++; hexagon: F1 dispersed in FaSSiF; triangle: F1 dispersed in HBSS++.

dissolved ABT-102 in our experiments has been quantified 20 h after dispersing the ASDs, while apparent solubility and permeation were determined one hour after dispersing the samples in medium. Since supersaturation is known to be a metastable state (Brouwers et al., 2009) our values may underestimate the extent of supersaturation.

## 5. Conclusion

The examined ASD enhanced in vitro permeation rate of ABT-102 across Caco-2-monolayers as compared to the crystalline drug. Enhanced permeation rate goes in parallel with increased concentration of molecularly dissolved ABT-102. In contrast, an even higher increase in apparent solubility due to micellarization neither affects concentration of molecularly dissolved ABT-102 nor permeation rate. To our understanding, the results reported here represent the first experimental proof that permeation rate enhancement in aqueous dispersions of ASDs is due to enhanced concentration of molecularly dissolved ABT-102 (“true” supersaturation) rather than enhanced apparent solubility in the presence of surfactants.

## Acknowledgements

We would like to thank Dr. Stephen Buckley for proof-reading of the manuscript and Abbott GmbH & Co. KG, D-67061 Ludwigshafen, Germany for financial support of this study.

## Appendix A. Supplementary data

Supplementary data associated with this article can be found, in the online version, at <http://dx.doi.org/10.1016/j.ijpharm.2012.08.014>.

## References

- Amidon, G.L., Lennernas, H., Shah, V.P., Crison, J.R., 1995. A theoretical basis for a biopharmaceutical drug classification: the correlation of in vitro drug product dissolution and in vivo bioavailability. *Pharm. Res.* **12**, 413–420.
- Becerra, N., Nuez, L.R.D., Zanocco, A.L., Lemp, E., 2006. Solubilization of dodac small unilamellar vesicles by sucrose esters: a fluorescence study. *Colloids Surf., A* **272**, 2–7.
- Breitenbach, J., 2002. Melt extrusion: from process to drug delivery technology. *J. Pharm. Biopharm.* **54**, 107–117.



- Brouwers, J., Brewster, M.E., Augustijns, P., 2009. Supersaturating drug delivery systems: the answer to solubility-limited oral bioavailability. *J. Pharm. Sci.* **98**, 2549–2572.
- Buch, P., Holm, P., Thomassen, J.Q., Scherer, D., Branscheid, R., Kolb, U., Langguth, P., 2010a. IVIVC for fenofibrate immediate release tablets using solubility and permeability as in vitro predictors for pharmacokinetics. *J. Pharm. Sci.* **99**, 4427–4436.
- Buch, P., Holm, P., Thomassen, J.Q., Scherer, D., Kataoka, M., Yamashita, S., Langguth, P., 2010b. IVIVR in oral absorption for fenofibrate immediate release tablets using dissolution and dissolution permeation methods. *Pharmazie* **65**, 723–728.
- Buckley, S.T., Fischer, S.M., Fricker, G., Brandl, M., 2012. In vitro models to evaluate the permeability of poorly soluble drug entities: challenges and perspectives. *Eur. J. Pharm. Sci.* **45**, 235–250.
- Cheng, C.-Y., Wank, J.-Y., Kausik, R., Lee, K.Y.C., Han, S., 2012. An ultrasensitive tool exploiting hydration dynamics to decipher weak lipid membrane-polymer interactions. *J. Magn. Reson.* **215**, 115–119.
- Dawson, R.M.C., Elliott, D.C., Elliott, W.H., 1989. Data for Biochemical Research. Clarendon Press.
- Do, T.T., Van Speybroeck, M., Mols, R., Annaert, P., Martens, J., Van Humbeeck, J., Vermant, J., Augustijns, P., Van den Mooter, G., 2011. The conflict between in vitro release studies in human biorelevant media and the in vivo exposure in rats of the lipophilic compound fenofibrate. *Int. J. Pharm.* **414**, 118–124.
- Fischer, S.M., Brandl, M., Fricker, G., 2011. Effect of the non-ionic surfactant Poloxamer 188 on passive permeability of poorly soluble drugs across Caco-2 cell monolayers. *Eur. J. Pharm. Biopharm.* **79**, 416–422.
- Frank, K.J., Westedt, U., Rosenblatt, K.M., Holig, P., Rosenberg, J., Magerlein, M., Brandl, M., Fricker, G., 2012. Impact of FaSSIF on the solubility and dissolution/permeation rate of a poorly water-soluble compound. *Eur. J. Pharm. Sci.* **47**, 16–20.
- Hubatsch, I., Ragnarsson, E.G., Artursson, P., 2007. Determination of drug permeability and prediction of drug absorption in Caco-2 monolayers. *Nat. Protoc.* **2**, 2111–2119.
- Ingels, F., Beck, B., Oth, M., Augustijns, P., 2004. Effect of simulated intestinal fluid on drug permeability estimation across Caco-2 monolayers. *Int. J. Pharm.* **274**, 221–232.
- Janssens, S., Van den Mooter, G., 2009. Review: physical chemistry of solid dispersions. *J. Pharm. Pharmacol.* **61**, 1571–1586.
- Kanzer, J., Tho, I., Flaten, G.E., Magerlein, M., Holig, P., Fricker, G., Brandl, M., 2010. In vitro permeability screening of melt extrudate formulations containing poorly water-soluble drug compounds using the phospholipid vesicle-based barrier. *J. Pharm. Pharmacol.* **62**, 1591–1598.
- Kym, P.R., Kort, M.E., Hutchins, C.W., 2009. Analgesic potential of TRPV1 antagonists. *Biochem. Pharmacol.* **78**, 211–216.
- Leuner, C., Dressman, J., 2000. Improving drug solubility for oral delivery using solid dispersions. *Eur. J. Pharm. Biopharm.* **50**, 47–60.
- Linn, M., Collnot, E.M., Djuric, D., Hempel, K., Fabian, E., Kolter, K., Lehr, C.M., 2012. Soluplus(R) as an effective absorption enhancer of poorly soluble drugs in vitro and in vivo. *Eur. J. Pharm. Sci.* **45**, 336–343.
- Miller, J.M., Beig, A., Carr, R.A., Spence, J.K., Dahan, A., 2012. A win-win solution in oral delivery of lipophilic drugs: supersaturation via amorphous solid dispersions increases apparent solubility without sacrifice of intestinal membrane permeability. *Mol. Pharmacol.*
- Overhoff, K.A., McConville, J.T., Yang, W., Johnston, K.P., Peters, J.I., Williams 3rd, R.O.J., 2008. Effect of stabilizer on the maximum degree and extent of supersaturation and oral absorption of tacrolimus made by ultra-rapid freezing. *Pharm. Res.* **25**, 167–175.
- Schwebel, H.J., van Hoogevest, P., Leigh, M.L., Kuentz, M., 2011. The apparent solubilizing capacity of simulated intestinal fluids for poorly water-soluble drugs. *Pharm. Dev. Technol.* **16**, 278–286.
- Singh, A., Worku, Z.A., Van den Mooter, G., 2011. Oral formulation strategies to improve solubility of poorly water-soluble drugs. *Expert Opin. Drug Delivery* **8**, 1361–1378.
- Van Speybroeck, M., Mellaerts, R., Mols, R., Thi, T.D., Martens, J.A., Van Humbeeck, J., Annaert, P., Van den Mooter, G., Augustijns, P., 2010a. Enhanced absorption of the poorly soluble drug fenofibrate by tuning its release rate from ordered mesoporous silica. *Eur. J. Pharm. Sci.* **41**, 623–630.
- Van Speybroeck, M., Mols, R., Mellaerts, R., Thi, T.D., Martens, J.A., Van Humbeeck, J., Annaert, P., Van den Mooter, G., Augustijns, P., 2010b. Combined use of ordered mesoporous silica and precipitation inhibitors for improved oral absorption of the poorly soluble weak base itraconazole. *Eur. J. Pharm. Biopharm.* **75**, 354–365.
- Vasconcelos, T., Sarmiento, B., Costa, P., 2007. Solid dispersions as strategy to improve oral bioavailability of poor water soluble drugs. *Drug Discovery Today* **12**, 1068–1075.

Q2

Q2

Q2

Q2

Q2

Q2

Q2

Q2

Q2